# Uptake of Organic Vapors and Nitric Acid on Atmospheric Freshly Nucleated Particles

Yosef Knattrup and Jonas Elm

Department of Chemistry, Aarhus University, Langelandsgade 140, 8000 Aarhus C, Denmark

**Correspondence:** Jonas Elm (jelm@chem.au.dk)

**Abstract.** Sulfuric acid, ammonia, and amines are believed to be key contributors to the initial steps in new particle formation in the atmosphere. However, other compounds such as organic compounds or nitric acid are believed to be important for further growth at larger sizes. In this study, we investigate the potential uptake of first-generation oxidation products from $\alpha$-pinene (pinic and pinonic acid), and isoprene (trans-$\beta$-IEPOX, $\beta$4-ISPOOH, and $\beta$1-ISOPOH), a potential highly oxidized molecule

5   (HOM), formic acid, and nitric acid. The uptake is probed onto $(SA)_{10}(base)_{10}$ freshly nucleated particles (FNPs), where SA denotes sulfuric acid and the bases are either ammonia (AM), methylamine (MA), dimethylamine (DMA), or trimethylamine (TMA). The addition free energies were calculated at the $\omega$B97X-D3BJ/6-311++G(3df,3pd)//B97-3c level of theory. We find favorable addition free energies of $-8$ to $-10$ kcal/mol for the HOM, pinic acid, and pinonic acid on the less sterically hindered $(SA)_{10}(AM)_{10}$ and $(SA)_{10}(MA)_{10}$ FNPs. This suggests that isoprene oxidation products do not contribute to the early growth

10   of FNPs, but the $\alpha$-pinene products do, in accordance with their expected volatilities.

    Calculating the second addition of a pinic acid molecule or pinonic acid molecule on the $(SA)_{10}(AM)_{10}$ FNPs, we find that pinic acid maintains its large addition free energy decrease due to its two carboxylic acid groups interacting with the other monomer as well as the FNP. The pinonic acid addition free energy drops to $-3.9$ kcal/mol due to the weak interactions between the FNP and its carbonyl group and the lack of monomer–monomer interactions. Calculating the addition free energy

15   under realistic atmospheric conditions, we find that the FNPs studied are too small (1.4 nm) to support the growth of the studied uptake monomers. We find that the accretion product pinyl diaterpenylic ester (PDPE, $C_{17}H_{26}O_8$) yields an uptake free energy value of -17.1 kcal/mol. This suggests that PDPE can overcome the strong Kelvin effect of a 1.4 nm FNP and lead to spontaneous uptake at ambient conditions.

## 1   Introduction

Clouds play a significant role in shaping the global climate and their formation begins when water condenses onto cloud condensation nuclei (CCN) (Boucher and Lohmann, 1995). Aerosols can act as CCN, delivering the required surface area for water to condense on, when they reach sizes of roughly 50–100 nm in diameter (Boucher and Lohmann, 1995). The

25   cloud–aerosol interaction is, as of the 5th IPCC assessment report, the largest cause of uncertainty in modern radiative forcing

modeling (Canadell et al., 2021). Aerosols form through two main pathways: either as primary particles, directly emitted into the atmosphere, or as secondary particles, which form through the clustering of gas vapors (Kulmala et al., 2013). Around 50% of CCN are believed to originate from the secondary process (Boucher and Lohmann, 1995; Merikanto et al., 2009) denoted new particle formation (NPF). As an example, Zhao et al. (2024) simulated the spatial distribution of CCN at the surface level and found the fraction of CCN from NPF to be around 30–40% over mainland Europe and up to $\approx 60\%$ over eastern United States.

The substantial uncertainty in the climate models is linked with the unidentified mechanisms for the NPF pathways and the early growth behavior of freshly nucleated particles (FNPs) (Canadell et al., 2021). For instance, Tröstl et al. (2016) found a factor two difference in predicted CCN number concentration, when altering the 1.7–3.0 nm particles growth mechanisms in their global model. It is therefore important to elucidate the initial growth mechanisms. Wang et al. (2020) found, experimentally, that vapors of ammonia (AM) and nitric acid (NA) could condense onto freshly nucleated particles (FNPs) at 278.5 K but temperatures below 258.15 K were required for nucleation of NA and AM. They extended this study (Wang et al., 2022) to include sulfuric acid (SA) and found that NA, SA, and AM could form particles in conditions similar to the upper free troposphere. Stolzenburg et al. (2018) studied the influence of organics in early particle growth in the CLOUD chamber and found rapid growth from organics in temperature ranges of 248.15–298.15 K.

Experimentally, the main focus has been on measuring particles larger than 2 nm in diameters, as particles below this size are challenging to measure accurately. Sub 2 nm charged cluster compositions have been measured by mass spectrometry techniques (Jokinen et al., 2012), however, it is uncertain if the measured clusters underwent fragmentation inside the instrument or if the charging of neutral clusters changes the composition during the measurement (Zapadinsky et al., 2019; Passananti et al., 2019). This positions quantum chemical methods as a key tool for exploring the formation of small clusters and their early growth processes.

The initial clustering process is believed to primarily be driven by sulfuric acid (SA) stabilized by ammonia (AM) (Kulmala et al., 2013; Kirkby et al., 2011; Schobesberger et al., 2013; Weber et al., 1996; Elm, 2021a; Dunne et al., 2016; Kubečka et al., 2023b) or strong amines such as methylamine (MA) (Kurtén et al., 2008; Nadykto et al., 2011, 2015, 2014; Jen et al., 2014; Glasoe et al., 2015; Kubečka et al., 2023b), dimethylamine (DMA) (Kurtén et al., 2008; Loukonen et al., 2010; Nadykto et al., 2011, 2015, 2014; Jen et al., 2014; Glasoe et al., 2015; Almeida et al., 2013; Elm, 2021a; Kubečka et al., 2023b) and trimethylamine (TMA) (Elm, 2021a; Kurtén et al., 2008; Nadykto et al., 2011; Jen et al., 2014; Nadykto et al., 2015; Glasoe et al., 2015; Kubečka et al., 2023b). Nitric acid (NA) (Wang et al., 2020; Liu et al., 2021, 2018; Kumar et al., 2018; Ling et al., 2017; Wang et al., 2022; Nguyen et al., 1997; Longsworth et al., 2023; Knattrup et al., 2023; Knattrup and Elm, 2022; Bready et al., 2022; Qiao et al., 2024) and formic acid (FA) (Bready et al., 2022; Knattrup et al., 2023; Ayoubi et al., 2023; Zhang et al., 2022, 2018; Harold et al., 2022; Nadykto and Yu, 2007) have also been shown to be involved in the initial clustering. Organics have not been definitively proven to take part in the initial clustering process but they are known to be important for the growth(Kulmala et al., 2013; Elm et al., 2020, 2023; Engsvang et al., 2023b).

While much of the focus has been on the initial clustering process (up to 8 monomers) (Elm et al., 2020, 2023; Engsvang et al., 2023b), Engsvang et al. (Engsvang et al., 2023a; Engsvang and Elm, 2022) and Wu et al. (Wu et al., 2023, 2024)

have pushed the studies up to large particles of up to 30–60 monomers, reaching geometric diameters of up to 2 nm, where the clusters start exhibiting more particle-like properties. Wu et al. (2024) defined the cluster-to-particle transition point as the point where the free energy per monomer starts leveling off, thereby resembling "bulk" thermodynamics and where "solvated" monomers appear in the cluster structures. They found this point to be around 10 acid-base pairs for the SA–AM/MA/DMA/TMA clusters and defined the clusters at and beyond this point as FNPs. Previously, DePalma et al. (2015) studied the uptake of pinic and pinonaldehyde on a $(SA)_4(AM)_4$ cluster at the AM1 level of theory. However, the early growth of realistic sizes $\sim$2 nm FNPs has yet to be studied.

In this paper, we study the uptake of NA and common organics (denoted X) on the $(SA)_{10}(AM/MA/DMA/TMA)_{10}$ FNPs using quantum chemical methods for the following reaction scheme:

$$(SA)_{10}(base)_{10} + (X)_1 \rightarrow (SA)_{10}(base)_{10}(X)_1 \tag{1}$$

We chose these sizes as the clusters have all reached the cluster-to-particle transition point. We investigate the first-generation oxidation products of $\alpha$-pinene, isoprene (Nozière et al., 2015) and a potential highly oxidized molecule (HOM) of $\alpha$-pinene (Kurtén et al., 2016) (suggested by COSMO-RS calculations). The studied systems are displayed in Figure 1.
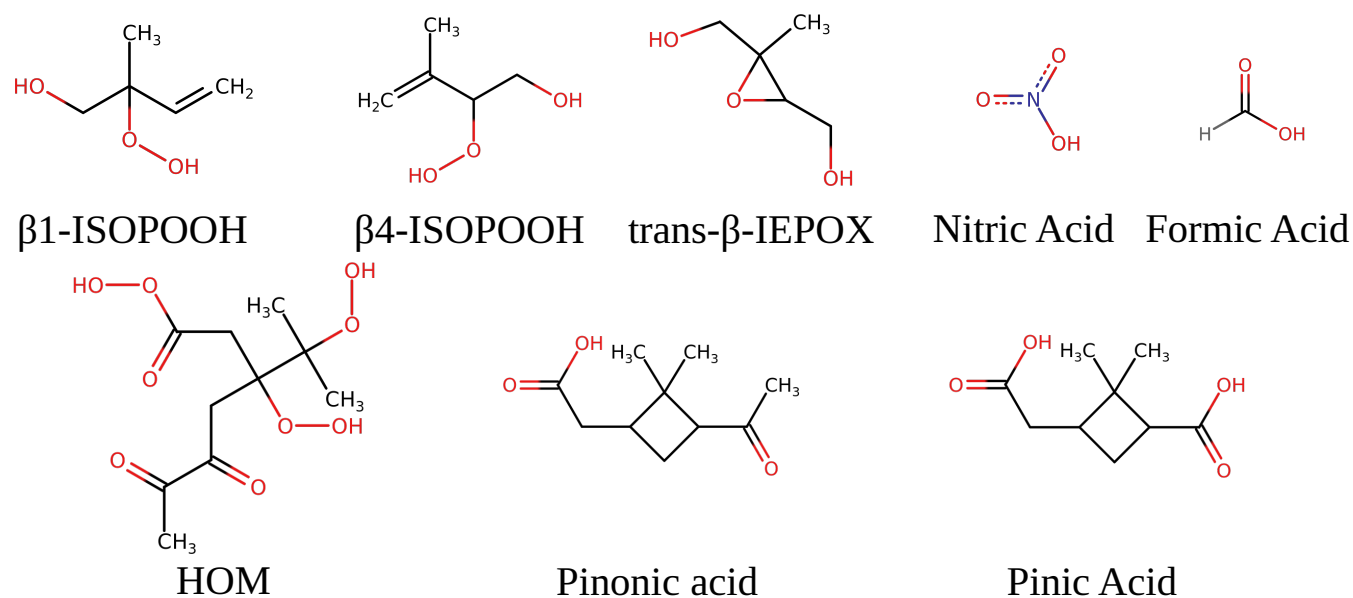
**Figure 1.** The molecular structure of the studied monomers. Pinonic and pinic acid are first-generation oxidation products from $\alpha$-pinene. trans-$\beta$-IEPOX, $\beta$4-ISOPOOH, and $\beta$1-ISOPOOH are first-generation oxidation product from isoprene.

## 2 Methodology

### 2.1 Computational Details

The B97-3c (Brandenburg et al., 2018) and $\omega$B97X-D3BJ (Najibi and Goerigk, 2018)/6-311++G(3df,3pd) (Ditchfield et al., 1971) calculations were performed in ORCA 5.0.4 (Neese, 2012; Neese et al., 2020; Neese, 2022). The xTB 6.4.0 (Bannwarth et al., 2021) program was used for the GFN1-xTB$^{\text{re-par}}$ calculations. GFN1-xTB$^{\text{re-par}}$ is a parameterization of GFN1-xTB (Grimme et al., 2017) using the methodology suggested by Knattrup et al. (2024). This specific parameterization was done by Wu et al. (2024) where a linear combination of the binding energy and gradient errors were minimized on a set of B97-3c FNPs. Configurational sampling was performed using ABCluster 3.2 (Zhang and Dolg, 2015, 2016; Zhang, 2022) and CREST 2.12 (Grimme, 2019; Pracht et al., 2020) in noncovalent interaction mode. The entire computational workflow and subsequent data handling was performed using the JKCS 2.1 suite of programs (Kubečka et al., 2023a). All the data is freely available in the atmospheric cluster database (Kubečka et al., 2023a; Elm, 2019). See the data availability section for more information.

### 2.2 Thermochemistry

We define the binding free energy $\Delta G_{\text{bind}}$ as the free energy change between the combined cluster ($G_{\text{cluster}}$), and the free energy ($G_{\text{monomer}}$) from the $n$ monomers,

$$\Delta G_{\text{bind}} = G_{\text{cluster}} - \sum_{i}^{n} G_{\text{monomer}}^{i}. \tag{2}$$

To get more accurate free energies, we performed a higher level single point correction on top of the DFT geometries. This is denoted with the sp//geo notation, where "sp" is the single point energy method used to calculate the electronic energy ($E^{\text{sp}}$), and "geo" is the method used to calculate the thermal correction to the free energy ($G_{\text{thermal}}^{\text{geo}}$) from the optimized structure and vibrational frequencies. The thermal correction term includes everything except the electronic energy:

$$G = E^{\text{sp}} + G_{\text{thermal}}^{\text{geo}}. \tag{3}$$

The addition free energy is the binding free energy change when a monomer is added to the cluster:

$$\Delta G_{\text{add}} = \Delta G_{\text{bind}}^{\text{cluster+uptake}} - \Delta G_{\text{bind}}^{\text{cluster}}. \tag{4}$$

We employ the quasi-harmonic approximation (Grimme, 2012) (as standard in ORCA), where vibrational frequencies below $100 \, \text{cm}^{-1}$ are treated as free rotor contributions to the entropy.

$$S_{\text{rot,qh}} = \frac{1}{2}R + R \ln \left[ \left( \frac{8\pi^3 I' k_{\text{B}} T}{h^2} \right)^{1/2} \right], \tag{5}$$

where $k_{\text{B}}$ is the Boltzmann constant, $T$ the temperature, $I'$ the effective moment of inertia, $R$ the gas constant, and $h$ is the Planck constant.

The output of quantum chemical programs are, for the most part, at standard conditions ($p = 1$ atm, $T = 298.15$ K). Changing the temperature can be done by reevaluating the standard statistical mechanics expressions at the wanted temperature. If the binding free energy is needed at other conditions, Halonen (2022) derived the following equation for the binding free energy at the given monomer concentrations,

$$\Delta G_{\text{bind}}(\boldsymbol{p}) = \Delta G_{\text{bind}}^{\text{ref}} - RT\left(1 - \frac{1}{n}\right)\sum_i^n \ln\left(\frac{p_i}{p_{\text{ref}}}\right), \tag{6}$$

where $p_i$ is the partial pressure (concentration) of monomer $i$, $n$ is the number of monomers, and $p_i$ is the reference pressure the reference binding free energy was calculated at. This equation correctly satisfies self-consistency for multi-component clusters (the monomers will have a free energy of zero) and the law of mass action. Combining Equation 6 with Equation 4 yields the addition free energy at the given conditions,

$$\Delta G_{\text{add}}(\boldsymbol{p}) = \Delta G_{\text{add}}^{\text{ref}} - \frac{RT}{n(n-1)}\left(\sum_i^{n-1}\ln\left(\frac{p_i}{p_{\text{ref}}}\right) + (n-1)^2\ln\left(\frac{p_{\text{add}}}{p_{\text{ref}}}\right)\right), \tag{7}$$

now $n$ is the total number of monomers in the largest cluster, $\Delta G_{\text{add}}^{\text{ref}}$ is the reference addition free energy, the sum runs over all monomers in the clusters before the addition, and $p_{\text{add}}$ is the pressure (concentration) of the added monomer.

## 2.3 Configurational Sampling Workflow

We employed the configurational workflow for FNPs as suggested by Wu et al. (2023, 2024).

$$\text{ABC} \xrightarrow{N=10,000} \text{xTB}^{\text{OPT}} \xrightarrow{N=10,000} \text{B97-3c}^{\text{SP}} \xrightarrow[\text{filter}]{N=1,000} \text{B97-3c}^{\text{PART OPT}} \xrightarrow[\text{filter}]{N=100} \text{B97-3c}^{\text{FULL OPT}} \tag{8}$$
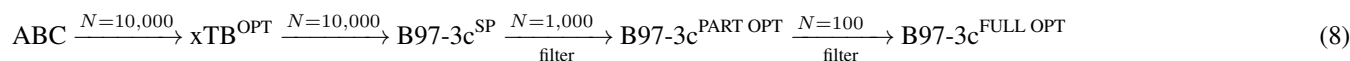
The workflow entails 10 parallel runs of ABCluster (Zhang and Dolg, 2015, 2016) with $SN = 1280$, $gen = 320$ and $sc = 4$. We used matching ionic monomers leading to an overall electronic neutral cluster. We choose to have ionic inorganic monomers and neutral organic monomers. We chose this because SA is a stronger acid compared to the monomers. All the structures from ABCluster are subsequently optimized with GFN1-xTB$^{\text{re-par}}$ and have a single point energy calculated at the B97-3c level of theory. The 1000 structures lowest in electronic energy are then partially optimized with B97-3c for 40 iterations. The 100 structures lowest in electronic energy are then fully optimized and, finally, a vibrational frequency calculation is performed.

The lowest free energy is used as the input structure for CREST using GFN1-xTB$^{\text{re-par}}$, as suggested by Knattrup et al. (2024), and the 100 structures lowest in electronic energy are then fully optimized followed by a vibrational frequency calculation.

$$\text{CREST(GFN1-xTB}^{\text{re-par}}) \xrightarrow{N=100} \text{B97-3c}^{\text{FULL OPT}} \tag{9}$$

The larger clusters suffered from memory issues and SCF convergence problems causing a low number of fully optimized structures using our automated workflow. We, therefore, restarted all 200 cluster calculations with increased memory and `VeryTightSCF`, and redid the CREST workflow, resulting in some cluster systems having over 200 configurations. The organic monomers were sampled using CREST. The ABCluster input was generated from the lowest energy conformer using topgen (Zhang, 2022; Zhang and Dolg, 2015, 2016) with charges from an MP2/6-31++G** calculation in Gaussian 16.

## 2.4 Single Point Refinement

Engsvang et al. (2023a) found that the B97-3c single point energies gave quite erroneous addition free energies for FNPs compared to the DLPNO-CCSD($T_0$)/aug-cc-pVTZ reference calculations. They found that $\omega$B97X-D3BJ/6-311++G(3df,3pd) had excellent error cancellation for the addition free energies yielding errors below 1 kcal/mol. Hasan et al. (2024) extended the benchmark by including single point calculations with $\omega$B97X-D3BJ and the augmented def2 basis sets. However, none managed to beat the combination found by Engsvang et al. (2023a) We, therefore, performed $\omega$B97X-D3BJ/6-311++G(3df,3pd) single point energy calculations on the 10 lowest free energy configurations. The SCF calculations had trouble converging due to linear dependencies in the basis, therefore, we had to increase the `scfthres` parameter to 1e-6. This change slightly increases the energy (max of 0.6 kcal/mol for the 10 acid 10 base systems), however, it is systematic for the given system size and should partly cancel out for the binding addition free energies.

It should be noted that the $\omega$B97X-D3BJ/6-311++G(3df,3pd) single point energies slightly overbind (roughly 4 kcal/mol) compared to the DLPNO-CCSD($T_0$)/aug-cc-pVTZ reference level by Engsvang et al. (2023a) However, all the energies are roughly shifted the same, leading to less erroneous addition free energies.

## 3 Results and Discussion

### 3.1 Addition Free Energies

To probe the potential for the $(SA)_{10}(AM/MA/DMA/TMA)_{10}$ FNPs to uptake monomers (pinic and pinonic acid, trans-$\beta$-IEPOX, $\beta$4-ISPOOH, $\beta$1-ISOPOOH), HOM, FA, and NA, we calculated the addition free energies as defined in equation (4).

The reference FNPs, without the uptake monomers, are taken from Wu et al. (2024). They found that for realistic atmospheric conditions ([SA] = $10^6$ molecules cm$^{-3}$, AM = (10 ppt, 10 ppb), MA/DMA/TMA = (1, 10 ppt)), the formation of the SA–AM and SA–MA FNPs go through nucleation barriers but are stable after the barrier. Furthermore, the formation of the SA–DMA FNP is found to be entirely barrierless but the formation of the SA–TMA FNP is unfavorable (due to sterical hindrance) as the binding free energy is positive for the studied conditions.

Figure 2 presents the calculated addition free energies, at the $\omega$B97X-D3BJ/6-311++G(3df,3pd)//B97-3c level of theory. It should be noted that the most negative binding free energy of the FNPs follows the order: MA > DMA > AM > TMA. This trend does not align with the gas-phase acidity or basicity of the components. Instead, steric factors become increasingly important for larger sizes, changing the order. In the following sections, we will discuss the trends for each FNP type.
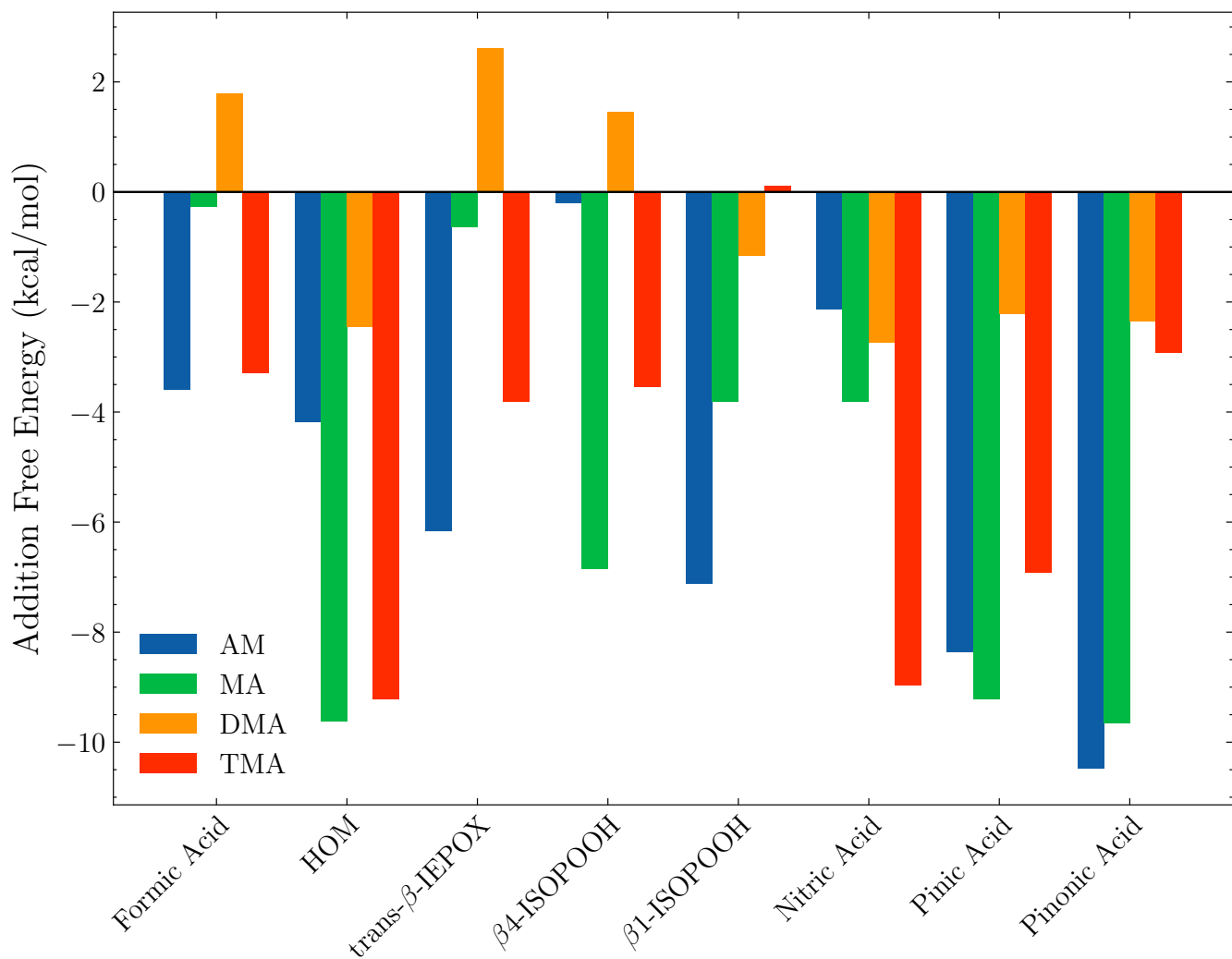
**Figure 2.** The addition free energy as defined in equation (4). The free energy is calculated using the lowest Gibbs free configuration (standard conditions) at the $\omega$B97X-D3BJ/6-311++G(3df,3pd)//B97-3c level of theory. The x-axis shows the monomer added to the $(SA)_{10}(base)_{10}$ FNP where the label defines the base.

### 3.1.1 SA–DMA

From Figure 2, it is seen that the $(SA)_{10}(DMA)_{10}$ FNPs are the least favorable for uptake of vapors, having positive addition free energies for FA, IEPOX, and $\beta4$-ISOPOOH and higher than $-3$ kcal/mol addition free energies for the remaining monomers. This is due to the several effects. First, SA–DMA FNPs are already substantially more stable than the other FNPs due to the high basicity of DMA compared to the other bases (Wu et al., 2024). Hence, the reference system in equation (4) is already low in free energy, leading to higher addition free energies. Second, the two bulky methyl groups in the DMA molecules

165 will lead to some steric hindrance when adding the organics to the FNP. Third, adding the new monomer disrupts the already favorable hydrogen bond network of the SA–DMA FNPs, by either destabilizing the system or only making it slightly more favorable. This concept is illustrated in Figure 3 for the $(SA)_{10}(DMA)_{10}(trans-\beta-IEPOX)_1$ structure. The addition of the IEPOX molecule forms an epoxide–DMA bond (light-blue circle), which forces the methyl group on the DMA molecule slightly inside the cluster, leading to increased steric repulsion. This is in contrast to the preferred orientation of the DMA molecule where

170 both methyl groups point out of the cluster (dark blue square).

## $(SA)_{10}(DMA)_{10}(trans-\beta-IEPOX)_1$

- ● Oxygen
- ● Nitrogen
- ● Carbon
- ○ Hydrogen
- ● Sulfur
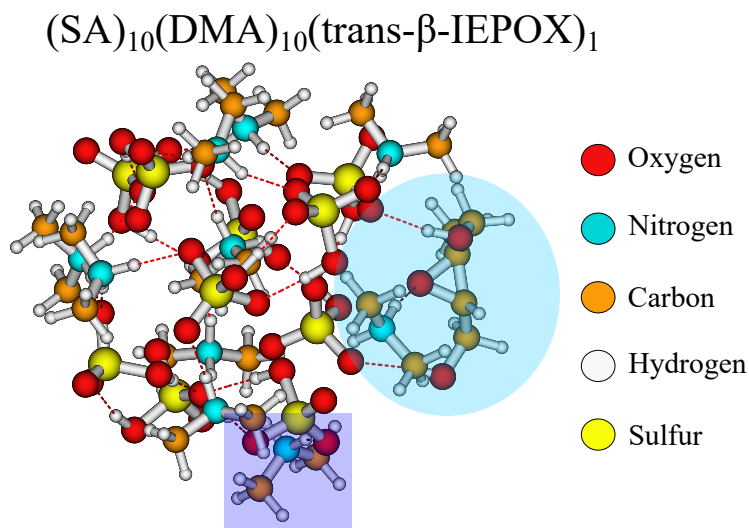
**Figure 3.** The $(SA)_{10}(DMA)_{10}(trans-\beta-IEPOX)_1$ cluster lowest in free energy (standard conditions) at the $\omega$B97X-D3BJ/6-311++G(3df,3pd)//B97-3c level of theory.

### 3.1.2 SA–TMA

For the $(SA)_{10}(TMA)_{10}$ FNPs, all the addition free energies are negative, except for $\beta$1-ISOPOOH (+0.1 kcal/mol). This is mainly caused by the fact that the SA–TMA FNPs by themselves are relatively unstable (Wu et al., 2024). Although TMA is

175 a stronger base, in terms of gas-phase basicity, (Hunter and Lias, 1998) than DMA, its three bulky methyl groups and only a single hydrogen bond donor prevents it from obtaining a favorable hydrogen bond topological network. Hence, introducing an additional monomer extends the hydrogen bond network and lowers the steric hindrance. It is curious that there is such a large difference between the two isomers of ISOPOOH (+0.1 vs −3.5 kcal/mol) as they structurally are very similar (see Figure 4). The geometries cannot easily explain the difference, as their carbon backbones point outwards from the cluster and

180 do not interact with the "core". This leaves the main cluster geometry as the driving parameter. Here, the $(SA)_{10}(TMA)_{10}(\beta$4-ISOPOOH$)_1$ cluster seems a bit less tightly packed compared to the $\beta$1-ISOPOOH cluster, which might equal a more favorable hydrogen bonding topological network.

$(SA)_{10}(TMA)_{10}(\beta 1\text{-ISOPOOH})_1$ $(SA)_{10}(TMA)_{10}(\beta 4\text{-ISOPOOH})_1$
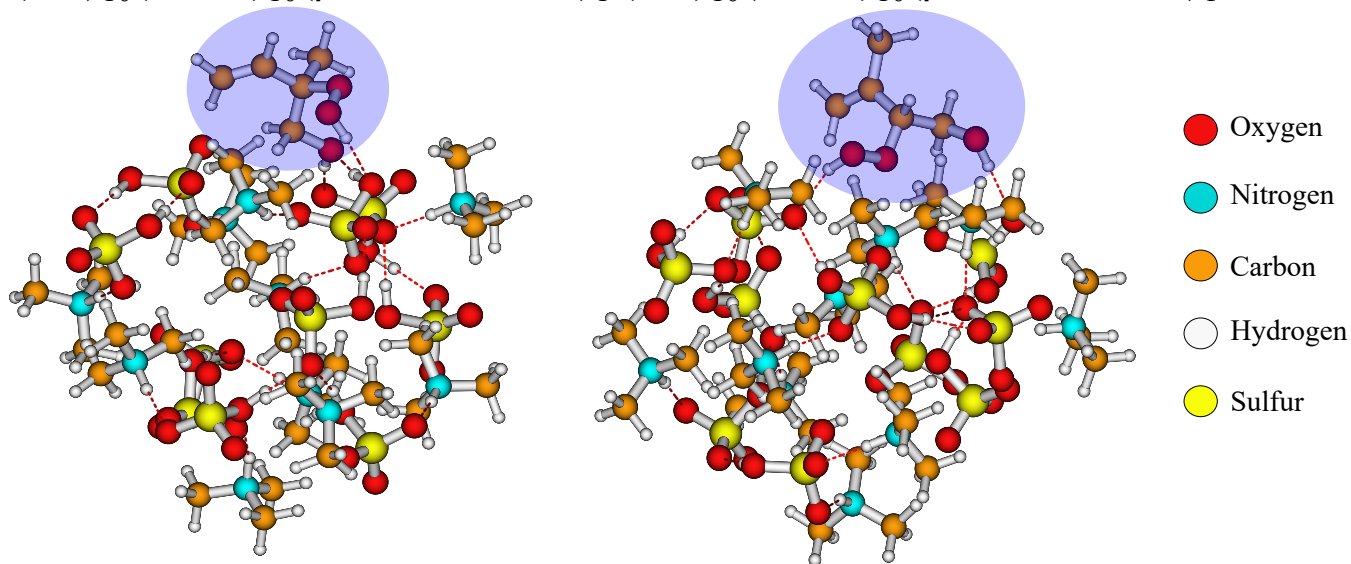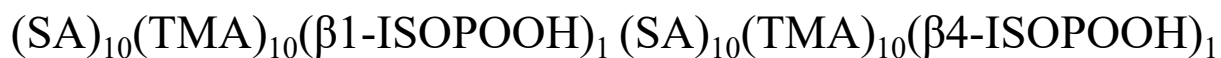
**Figure 4.** The $(SA)_{10}(TMA)_{10}(\beta 1\text{-ISOPOOH})_1$ and $(SA)_{10}(TMA)_{10}(\beta 4\text{-ISOPOOH})_1$ cluster lowest in free energy (standard conditions) at the $\omega$B97X-D3BJ/6-311++G(3df,3pd)//B97-3c level of theory.

Likewise, it is also curious that the bulky HOM has addition free energy in similar magnitudes ($-9.2$ kcal/mol) as the much
185    smaller nitric acid ($-9.0$ kcal/mol) and pinic acid ($-6.9$ kcal/mol). Studying the structure (Figure 5), the HOM appears to compress the entire cluster, "hovering" slightly above the surface, favoring internal hydrogen bonding as seen on the top of the HOM. This means that, while the first addition is very favorable, the second addition of another HOM is less likely, as this would potentially compress the cluster even further. However, the internal hydrogen bonds in the HOM could potentially be broken to act as a tether between two adjacent clusters.
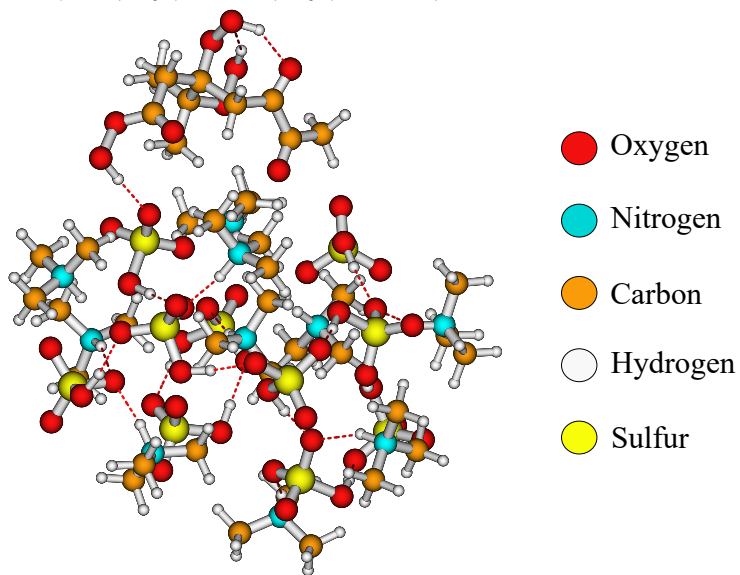
# (SA)$_{10}$(TMA)$_{10}$(HOM)$_1$

**Figure 5.** The (SA)$_{10}$(TMA)$_{10}$(HOM)$_1$ cluster lowest in free energy (standard conditions) at the $\omega$B97X-D3BJ/6-311++G(3df,3pd)//B97-3c level of theory.

### 3.1.3 SA–MA

The SA–MA FNPs have a notable negative addition free energy for the HOM ($-9.6$ kcal/mol), pinic ($-9.2$ kcal/mol) and pinonic acid ($-9.7$ kcal/mol). It is interesting that they are almost equivalent, as pinic acid has two carboxylic acid groups, whereas in pinonic acid one of the carboxylic acid groups is exchanged for a carbonyl group, and we would expect carboxylic acid to bind stronger.
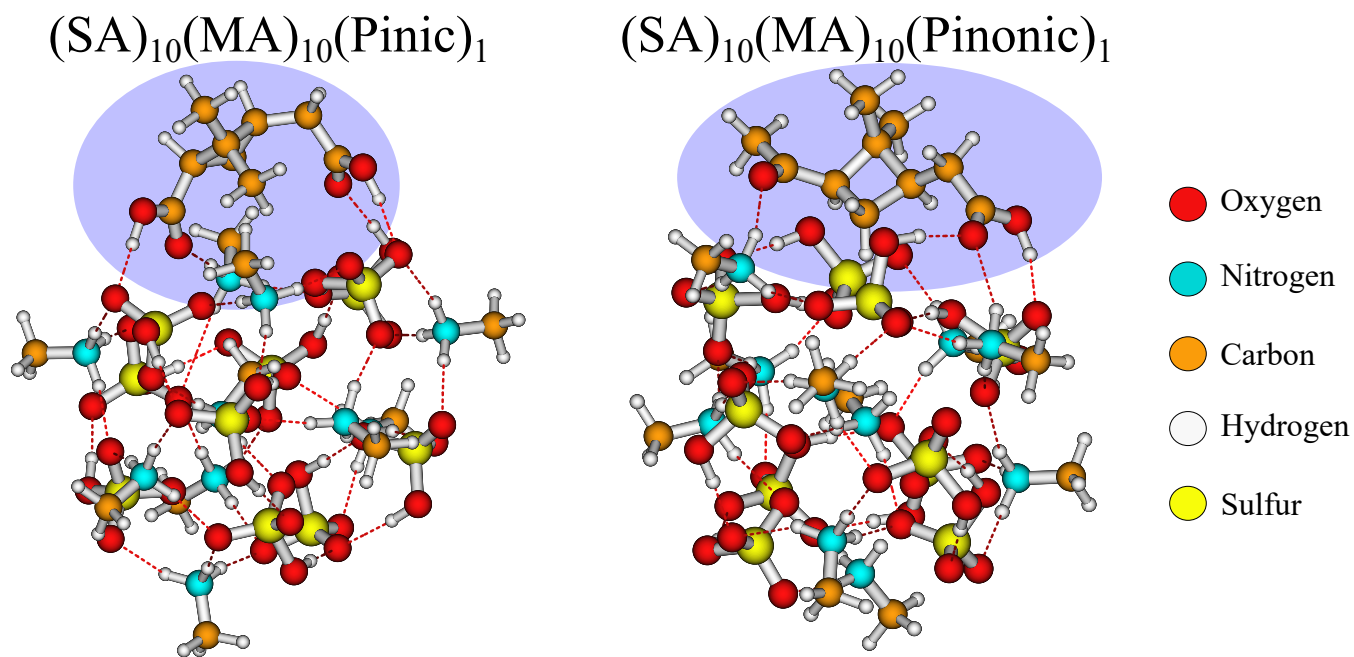
**Figure 6.** The $(SA)_{10}(MA)_{10}(Pinic)_1$ and $(SA)_{10}(MA)_{10}(Pinonic)_1$ cluster lowest in free energy (standard conditions) at the $\omega$B97X-D3BJ/6-311++G(3df,3pd)//B97-3c level of theory.

Studying the structures (Figure 6), we see they reside at the surface of the cluster, interacting with their carboxylic acid/carbonyl group in almost the same way. This suggests the clusters can rearrange to accommodate both types of interactions, and it does not matter much that one of the carboxylic acid groups has been exchanged with a carbonyl group.

$(SA)_{10}(MA)_{10}(HOM)_1$

Oxygen
Nitrogen
Carbon
Hydrogen
Sulfur
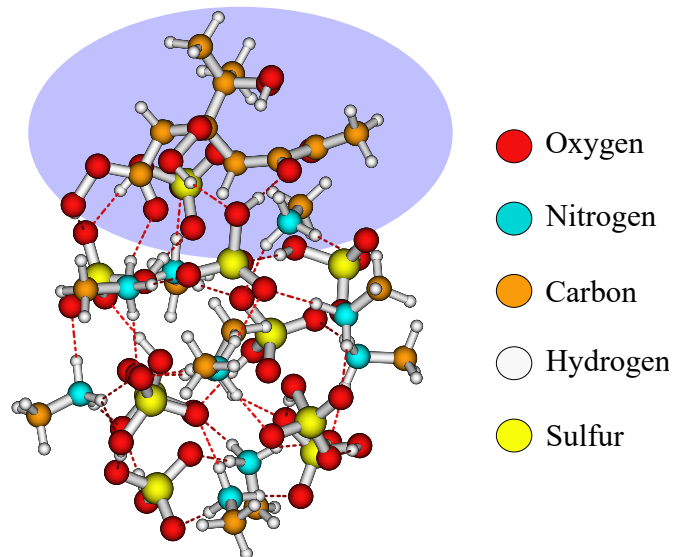
**Figure 7.** The $(SA)_{10}(MA)_{10}(HOM)_1$ cluster lowest in free energy (standard conditions) at the $\omega$B97X-D3BJ/6-311++G(3df,3pd)//B97-3c level of theory.

Like the SA–TMA cluster, it is quite favorable to add the HOM ($-9.6$ kcal/mol) but, unlike the SA–TMA structure, this matches chemical intuition as the HOM almost maximizes the interactions with the cluster as seen in Figure 7. This also fits with the interaction pattern of pinic and pinonic acid explaining the magnitude of the addition free energy.

### 3.1.4   SA–AM

The SA–AM FNPs have a similar negative addition free energy for pinic ($-8.4$ kcal/mol) and pinonic acid ($-10.5$ kcal/mol) as the SA–AM FNP. They also have the same structural characteristics. However, there is an inverse trend for the remaining monomers (FA, HOM, trans-$\beta$-IEPOX, $\beta$4-ISOPOOH, $\beta$1-ISOPOOH, and NA), where, if the addition free energy is substantially negative for one type of FNP, it is small for the other type of FNP, for a given monomer. This is especially noticeable for the $\beta$4-ISOPOOH monomer, where the addition free energy is almost zero for the SA–AM FNP, but $\approx -7$ kcal/mol for the SA–MA FNP. Structurally, it is unclear why the addition free energy differs so much, as both interact with the cluster's outer layer, and neither of their "backbone" carbon chains interact with the cluster (Figure 8, ISOPOOH has been marked with a dark blue box). The only major difference is that, in the SA–AM FNP, the dihedral angle between the two functional groups in ISOPOOH allows it to attach entirely to the surface, while for the SA–MA FNP, the dihedral angle between the functional groups causes it to be slightly more embedded in the cluster.

$(SA)_{10}(MA)_{10}(\beta4\text{-ISOPOOH})_1$  $(SA)_{10}(AM)_{10}(\beta4\text{-ISOPOOH})_1$

- ● Oxygen
- ● Nitrogen
- ● Carbon
- ○ Hydrogen
- ● Sulfur
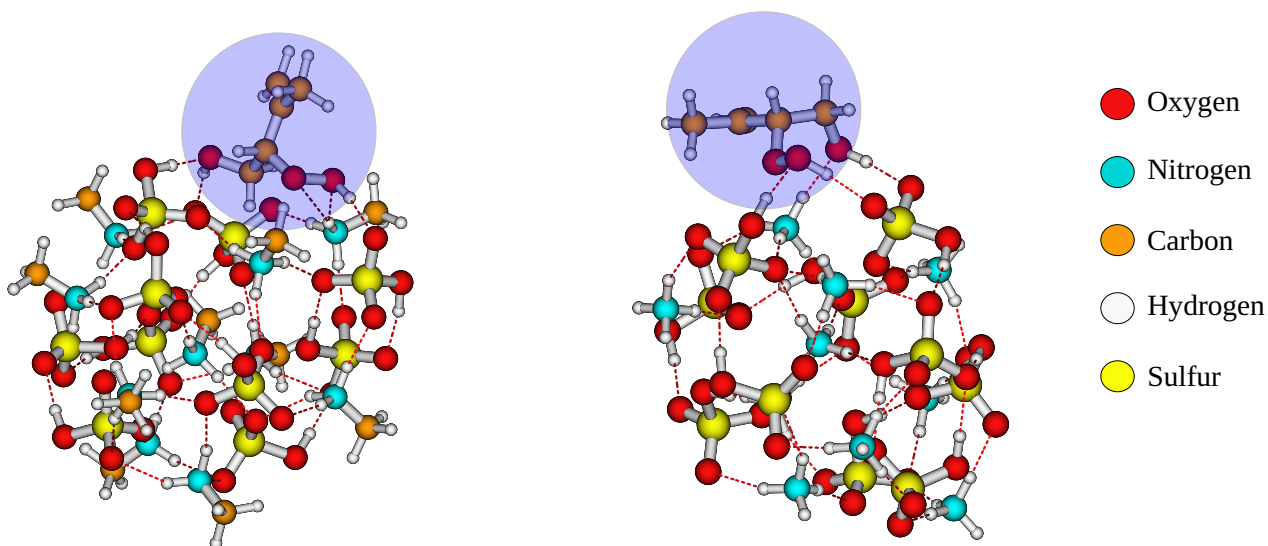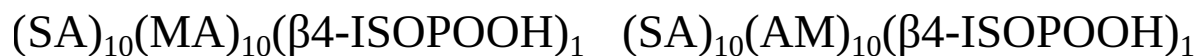
**Figure 8.** The $(SA)_{10}(MA)_{10}\beta4\text{-ISPOOH})_1$ and $(SA)_{10}(AM)_{10}\beta4\text{-ISPOOH})_1$ cluster lowest in free energy (standard conditions) at the $\omega$B97X-D3BJ/6-311++G(3df,3pd)//B97-3c level of theory.

### 3.2 Potential for Organic Growth

It is clear that FNPs containing 10 acid–base pairs might have the potential to grow via organic uptake, as we observed addition free energies below $-8$ kcal/mol for the HOM, pinic acid, and pinonic acid. It appears that isoprene oxidation products have a lower potential for contributing to early growth, compared to the $\alpha$-pinene products. This is in accordance with the expected vapor pressure of the compounds.

Out of the studied organic compounds, the HOM, pinic, and pinonic acid seem to be the most likely candidates for organic growth. To further investigate this, we calculated the addition free energy of a second pinic and pinonic acid molecule. We chose to study the SA–AM FNP, as it showed a large potential for uptake of these species.
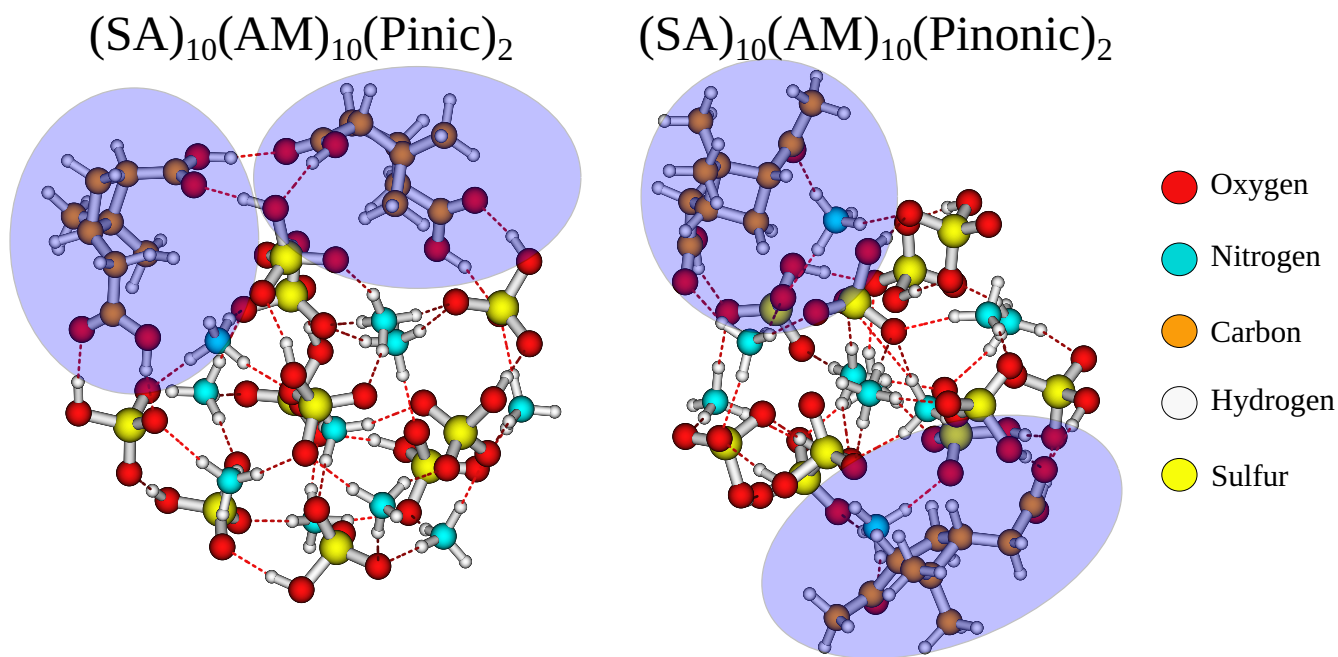
**Figure 9.** The $(SA)_{10}(AM)_{10}(Pinic)_2$ and $(SA)_{10}(AM)_{10}(Pinonic)_2$ cluster lowest in free energy (standard conditions) at the $\omega$B97X-D3BJ/6-311++G(3df,3pd)//B97-3c level of theory.

225    The addition free energy of the second addition is $-11.8$ and $-3.9$ kcal/mol for pinic and pinonic acid, respectively. The addition free energy of pinic acid is even lower than the first ($-8.4$ kcal/mol). On the contrary, the addition free energy of the second pinonic acid increased dramatically from the first addition ($-10.5$ kcal/mol). This stark contrast can easily be seen from the geometries in Figure 9. Pinic acid, with its two carboxylic acid groups, cannot only bind with the surface of the FNP but also with the other pinic acid. One could envision that with further additions of pinic acid molecules, they could link

230    together over the entire surface essentially leading to a core-shell structure. In contrast, pinonic acid only has one carboxylic acid group which attaches to the surface, However, it does not link the two monomers together as the carbonyl groups favors binding with the bases in the FNP. This is in agreement with the earlier findings by Elm et al. (2017) and the cluster-of-functional groups approach by Pedersen et al. (2024) which states that carboxylic acid groups yield the most negative addition free energy for organic enhanced atmospheric cluster formation. The fact that the organic–organic interaction is affecting the

235    FNP growth is an intriguing result. This could indicate that uptake of organics on small particles, and in extension the growth thermodynamics, significantly deviate from the usually employed metric of the saturation vapor pressure of the organics. Hence, uptake of organics might be as dependent on simultaneously the organic–organic interactions as the organic–FNP interactions. This implies that co-condensation of various vapors on FNPs will dependent strongly on the exact functional groups in the molecules and should be further studied in the future.

## 3.3 Free Energies Under Actual Conditions

The free energies calculated in the previous sections are under standard conditions ($p = 1$ atm, $T = 298.15$ K). However, as none of the species involved are present in such high concentrations in the atmosphere, the sign of the standard free energy change alone does not determine whether the addition is spontaneous under atmospheric conditions. To explore this, we scanned the free energy dependence on temperature and monomer concentration for the addition of pinic acid onto the $(SA)_{10}(AM/MA)_{10}$ FNPs. These systems were chosen because they showed favorable standard free energy changes for the first (and second, in the case of AM) addition. Two concentration regimes for the FNP components were selected based on the *Clusteromics* series of papers (Elm, 2021a, b, 2022; Knattrup and Elm, 2022; Ayoubi et al., 2023). For both regimes, SA is set to $10^6$ molecules cm$^{-3}$, the concentrations of bases were AM (10 ppt, 10 ppb), MA (1, 100 ppt) and DMA/TMA (1, 10 ppt) for the lower and upper regimes, respectively. Ambient pinic acid concentrations were assumed to range from 0.5 ppt to 20.5 ppt.
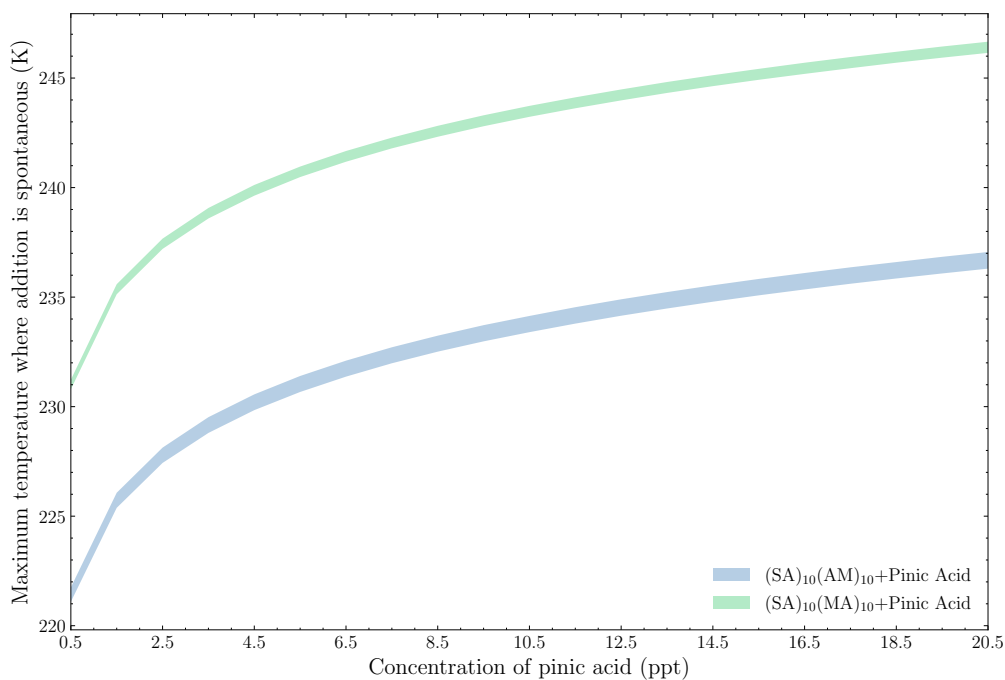
**Figure 10.** The maximum temperature where the addition of pinic acid onto either $(SA)_{10}(AM)_{10}$ or $(SA)_{10}(MA)_{10}$ is spontaneous at the given conditions ranging from the upper to the lower concentration regime the bases (Top of distribution = upper concentration regime, bottom of distribution = lower concentration regime).

Figure 10 shows the maximum temperature at which the addition of pinic acid to either $(SA)_{10}(AM)_{10}$ or $(SA)_{10}(MA)_{10}$ becomes spontaneous across these concentration regimes.

In general, the primary factor determining the spontaneity of addition is the concentration of pinic acid rather than the concentration of the FNP compounds. Increasing the pinic acid concentration from 0.5 ppt to 20 ppt raises the maximum

**15**

spontaneous condensation temperature from 221 K to 236 K for the addition onto the SA–AM FNP and from 231 K to 246 K for the addition onto the SA–MA FNP. Conversely, changing the base concentrations from the lower to the upper limits results in, at most, a 1 K difference. These findings suggest that pinic acid uptake is unlikely, even for the median concentration of 10 ppt, as it requires a temperature of 243 K for spontaneous addition onto the AM FNP. The addition to the MA FNP, however, is more favorable due to the direct proportionality between the addition temperature and the free energy change (Equation (7)). In the studied concentration range, the roughly 0.8 kcal/mol difference in addition free energy for the AM FNP compared to MA FNP results in a 10 K increase in the condensation temperature. Hence, the results are quite sensitive to the calculated free energies.

The NA and FA uptake onto the $(SA)_{10}(AM)_{10}$ FNP stands out compared to the other monomers, as their higher atmospheric concentrations (ppb rather than ppt) may allow spontaneous uptake, despite their standard addition free energy exceeding $-4$ kcal/mol. However, even at high concentrations (20.5 ppb) in the upper concentration regime, spontaneous addition of FA and NA requires temperatures below 209 K and 174 K, respectively. This is due to the logarithmic dependence of the free energy on concentration (from Equation (7)), which minimizes the temperature increase when shifting from ppt to ppb.

These temperatures are significantly colder than those reported in CLOUD chamber experiments by Wang et al. (2020) and Wang et al. (2022), where upper tropospheric conditions were sufficient for NA condensation. However, their experiments measured particles larger than 2 nm, whereas our SA–AM FNP is only 1.4 nm. These results suggest that monomer uptake cannot overcome the Kelvin effect for the studied FNP sizes under realistic conditions. Nonetheless, pinic acid remains the most promising candidate for spontaneous condensation onto larger FNPs under cold, but plausible, atmospheric conditions.

Another way to increase the probability of uptake is to increase the number of interacting groups in the uptake monomers. The cluster-of-functional groups approach by Pedersen et al. (2024), states that the binding free energies of organics can as a first approximation be estimated by their functional groups. For uptake on the $(SA)_{10}(AM)_{10}$ FNP, an organic with the functional groups of pinic acid ($-8.4$ kcal/mol) and pinonic acid ($-10.5$ kcal/mol) would give roughly $-19$ kcal/mol. The accretion product pinyl diaterpenylic ester (PDPE) (Kristensen et al., 2013, 2016) has three carboxylic and one ester group and should approximately function as pinonic and pinic acid combined (See Figure 11). The addition free energy for PDPE on the $(SA)_{10}(AM)_{10}$ FNP is $-17.1$ kcal mol$^{-1}$, and the structure is depicted in Figure 11.

Pinyl diaterpenylic ester

$(SA)_{10}(AM)_{10}(PDPE)_1$

- ● Oxygen
- ● Nitrogen
- ● Carbon
- ○ Hydrogen
- ● Sulfur
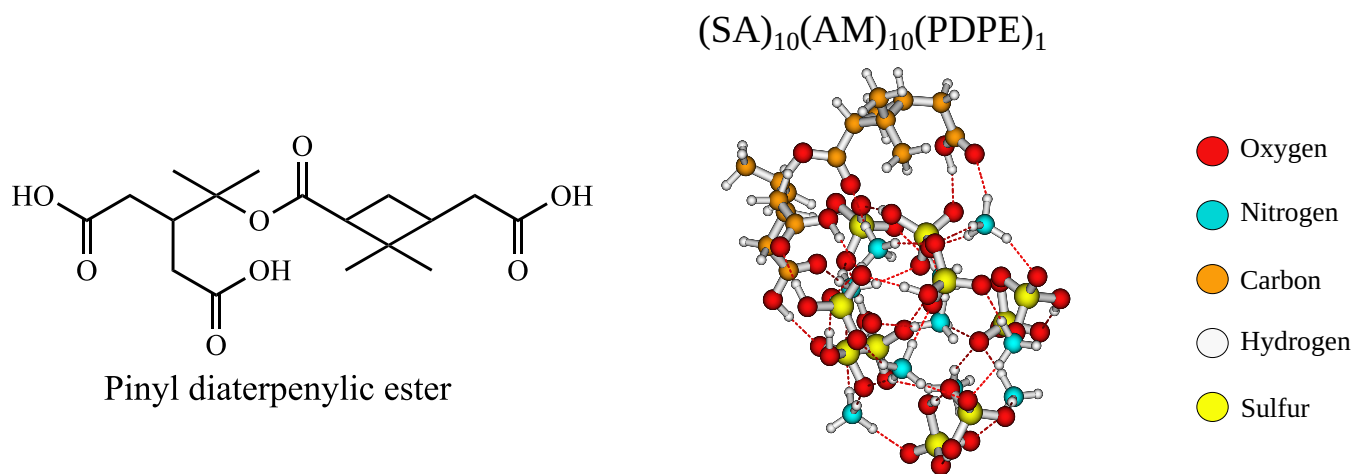
280

**Figure 11.** The structure and lowest Gibbs free configuration of the $(SA)_{10}(AM)_{10}(PDPE)_1$ FNP at the $\omega$B97X-D3BJ/6-311++G(3df,3pd)//B97-3c level of theory.

Calculating the free energy under given conditions in the upper concentration regime of FNP constituents, we find that for a concentration of 0.3 ppt for PDPE, the uptake is spontaneous at 298.15 K. At 0.03 ppt, the uptake is spontaneous at 278.15 K. This suggests that the extremely low volatile accretion products can overcome the Kelvin effect for FNPs at these sizes, but the low volatile monomer oxidation products cannot.

285  **4   Conclusions**

We have investigated the ability of $(SA)_{10}(base)_{10}$ freshly nucleated particles (FNPs) with SA = sulfuric acid and base = ammonia (AM), methylamine (MA), dimethylamine (DMA), and trimethylamine (TMA) to uptake first-generation oxidation products of isoprene (trans-$\beta$-IEPOX, $\beta$4-ISPOOH, and $\beta$1-ISOPOH), $\alpha$-pinene (pinic and pinonic acid), a potential highly oxidized molecule (HOM), formic acid (FA), and nitric acid (NA). This was done using quantum chemical methods at the
290  $\omega$B97X-D3BJ/6-311++G(3df,3pd)//B97-3c level of theory.

We find that the HOM, pinic, and pinonic acid can exhibit large decreases in addition free energies between $-8$ to $-10$ kcal/mol making them potential candidates for the organic growth of FNPs. This suggests that the studied isoprene oxidation products do not contribute to the early growth of FNPs, but the $\alpha$-pinene products do. To further investigate this we calculated the second addition free energy of pinic and pinonic acid onto the $(SA)_{10}(AM)_{10}$ FNP. We find that the pinic acid still exhibits a large
295  addition free energy decrease of $-11.8$ kcal/mol but the secondary addition of pinonic acid drops to $-3.9$ kcal/mol. The reason pinic acid maintains its high addition free energy decrease is due to its two carboxylic acid groups. The functional groups enable the pinic acid monomer to bind not only to the FNP surface but also to adjacent pinic acid. Calculating the addition free energy under realistic atmospheric conditions, we find that the FNPs studied are too small to support the growth of the studied monomer compounds, and extremely low volatile accretion products are required for spontaneous uptake on the studied FNPs.

300    In the future, we imagine molecular dynamics-based sampling techniques, such as umbrella sampling, can give better insight into the effects of multiple minima and partitioning of the uptake or collision simulations using molecular dynamics for realistic collision coefficients. It would also be interesting to study whether organic compounds can influence the cluster-to-particle transition points.

*Data availability.*  All the calculated structures and thermochemistry are available in the Atmospheric Cluster Database (ACDB) (Elm, 2019;
305    Kubečka et al., 2023a).

*Author contributions.*  Conceptualization: J.E.;
Methodology: Y.K., J.E.;
Formal analysis: Y.K.;
Investigation: Y.K.;
310    Resources: J.E.;
Writing - original draft: Y.K.;
Writing - review & editing: Y.K., J.E.;
Visualization: Y.K.;
Project administration: J.E.;
315    Funding acquisition: J.E;
Supervision: J.E.

*Competing interests.*  At least one of the (co-)authors is a member of the editorial board of Aerosol Research. The authors have no other competing interests to declare.

*Acknowledgements.*  Funded by the European Union (ERC, ExploreFNP, project 101040353). Views and opinions expressed are however
320    those of the authors only and do not necessarily reflect those of the European Union or the European Research Council Executive Agency. Neither the European Union nor the granting authority can be held responsible for them.

This work was funded by the Danish National Research Foundation (DNRF172) through the Center of Excellence for Chemistry of Clouds.

The numerical results presented in this work were obtained at the Centre for Scientific Computing, Aarhus https://phys.au.dk/forskning/
325    faciliteter/cscaa/.

# References

Almeida, J., Schobesberger, S., Kürten, A., Ortega, I. K., Kupiainen-Määttä, O., Praplan, A. P., Adamov, A., Amorim, A., Bianchi, F., Breitenlechner, M., and et al.: Molecular understanding of sulphuric acid–amine particle nucleation in the atmosphere, Nature, 502, 359–363, https://doi.org/10.1038/nature12663, 2013.

Ayoubi, D., Knattrup, Y., and Elm, J.: Clusteromics V: Organic Enhanced Atmospheric Cluster Formation, ACS Omega, 8, 9621–9629, https://doi.org/10.1021/acsomega.3c00251, 2023.

Bannwarth, C., Caldeweyher, E., Ehlert, S., Hansen, A., Pracht, P., Seibert, J., Spicher, S., and Grimme, S.: Extended Tight-Binding Quantum Chemistry Methods, WIREs Comput. Mol. Sci., 11, e1493, https://doi.org/10.1002/wcms.1493, 2021.

Boucher, O. and Lohmann, U.: The Sulfate-CCN-Cloud Albedo Effect, Tellus B: Chem. Phys. Meteorol., pp. 281–300, https://www.tandfonline.com/doi/abs/10.3402/tellusb.v47i3.16048, 1995.

Brandenburg, J. G., Bannwarth, C., Hansen, A., and Grimme, S.: B97-3c: A Revised Low-Cost Variant of the B97-D Density Functional Method, J. Chem. Phys., 148, 064 104, https://doi.org/10.1063/1.5012601, 2018.

Bready, C. J., Fowler, V. R., Juechter, L. A., Kurfman, L. A., Mazaleski, G. E., and Shields, G. C.: The Driving Effects of Common Atmospheric Molecules for Formation of Prenucleation Clusters: The Case of Sulfuric acid, Formic acid, Nitric acid, Ammonia, and Dimethyl Amine, Environ. Sci.: Atmos., 2, 1469–1486, https://doi.org/10.1039/D2EA00087C, 2022.

Canadell, J. G., Monteiro, P. M. S., Costa, M. H., Cotrim da Cunha, L., Cox, P., Eliseev, A. V., Henson, S., Ishii, M., Jaccard, S., Koven, C., and et al.: Global Carbon and other Biogeochemical Cycles and Feedbacks, pp. 673–816, Cambridge University Press, Cambridge, United Kingdom and New York, NY, USA, 2021.

DePalma, J. W., Wang, J., Wexler, A. S., and Johnston, M. V.: Growth of Ammonium Bisulfate Clusters by Adsorption of Oxygenated Organic Molecules, J. Phys. Chem. A, 119, 11 191–11 198, https://doi.org/10.1021/acs.jpca.5b07744, 2015.

Ditchfield, R., Hehre, W. J., and Pople, J. A.: Self-Consistent Molecular-Orbital Methods. IX. An Extended Gaussian-Type Basis for Molecular-Orbital Studies of Organic Molecules, J. Chem. Phys., 54, 724–728, https://doi.org/10.1063/1.1674902, 1971.

Dunne, E. M., Gordon, H., Kürten, A., Almeida, J., Duplissy, J., Williamson, C., Ortega, I. K., Pringle, K. J., Adamov, A., Baltensperger, U., and et al.: Global Atmospheric Particle Formation from CERN CLOUD Measurements, Science, 354, 1119–1124, https://doi.org/10.1126/science.aaf2649, 2016.

Elm, J.: An Atmospheric Cluster Database Consisting of Sulfuric Acid, Bases, Organics, and Water, ACS Omega, 4, 10 965–10 974, https://doi.org/10.1021/acsomega.9b00860, 2019.

Elm, J.: Clusteromics I: Principles, Protocols, and Applications to Sulfuric Acid–Base Cluster Formation, ACS Omega, 6, 7804–7814, https://doi.org/10.1021/acsomega.1c00306, 2021a.

Elm, J.: Clusteromics II: Methanesulfonic Acid–Base Cluster Formation, ACS Omega, 6, 17 035–17 044, https://doi.org/10.1021/acsomega.1c02115, 2021b.

Elm, J.: Clusteromics III: Acid Synergy in Sulfuric Acid–Methanesulfonic Acid–Base Cluster Formation, ACS Omega, 7, 15 206–15 214, https://doi.org/10.1021/acsomega.2c01396, 2022.

Elm, J., Myllys, N., and Kurtén, T.: What Is Required for Highly Oxidized Molecules To Form Clusters with Sulfuric Acid?, J. Phys. Chem. A, 121, 4578–4587, https://doi.org/10.1021/acs.jpca.7b03759, 2017.

Elm, J., Kubečka, J., Besel, V., Jääskeläinen, M. J., Halonen, R., Kurtén, T., and Vehkamäki, H.: Modeling the Formation and Growth of Atmospheric Molecular Clusters: A Review, J. Aerosol Sci., 149, 105 621, https://doi.org/10.1016/j.jaerosci.2020.105621, 2020.

Elm, J., Ayoubi, D., Engsvang, M., Jensen, A. B., Knattrup, Y., Kubečka, J., Bready, C. J., Fowler, V. R., Harold, S. E., Longsworth, O. M., and Shields, G. C.: Quantum Chemical Modeling of Organic Enhanced Atmospheric Nucleation: A Critical Review, WIREs Comput. Mol. Sci., 13, e1662, https://doi.org/10.1002/wcms.1662, 2023.

365

Engsvang, M. and Elm, J.: Modeling the Binding Free Energy of Large Atmospheric Sulfuric Acid–Ammonia Clusters, ACS Omega, 7, 8077–8083, https://doi.org/10.1021/acsomega.1c07303, 2022.

Engsvang, M., Kubečka, J., and Elm, J.: Toward Modeling the Growth of Large Atmospheric Sulfuric Acid–Ammonia Clusters, ACS Omega, 8, 34 597–34 609, https://doi.org/10.1021/acsomega.3c03521, 2023a.

370

Engsvang, M., Wu, H., Knattrup, Y., Kubečka, J., Jensen, A. B., and Elm, J.: Quantum Chemical Modeling of Atmospheric Molecular Clusters Involving Inorganic Acids and Methanesulfonic Acid, Chem. Phys. Rev., 4, 031 311, https://doi.org/10.1063/5.0152517, 2023b.

Glasoe, W. A., Volz, K., Panta, B., Freshour, N., Bachman, R., Hanson, D. R., McMurry, P. H., and Jen, C.: Sulfuric acid Nucleation: An Experimental Study of the Effect of Seven Bases, J. Geophys. Res. Atmos., 120, 1933–1950, https://doi.org/10.1002/2014JD022730, 2015.

375

Grimme, S.: Supramolecular Binding Thermodynamics by Dispersion-Corrected Density Functional Theory, Chem. Eur. J., 18, 9955–9964, https://doi.org/10.1002/chem.201200497, 2012.

Grimme, S.: Exploration of Chemical Compound, Conformer, and Reaction Space with Meta-Dynamics Simulations Based on Tight-Binding Quantum Chemical Calculations, J. Chem. Theory Comput., 15, 2847–2862, https://doi.org/10.1021/acs.jctc.9b00143, 2019.

Grimme, S., Bannwarth, C., and Shushkov, P.: A Robust and Accurate Tight-Binding Quantum Chemical Method for Structures, Vibrational

380

Frequencies, and Noncovalent Interactions of Large Molecular Systems Parametrized for All spd-Block Elements (Z = 1–86), J. Chem. Theory Comput., 13, 1989–2009, https://doi.org/10.1021/acs.jctc.7b00118, 2017.

Halonen, R.: A Consistent Formation Free Energy Definition for Multicomponent Clusters in Quantum Thermochemistry, J. Aerosol Sci., 162, 105 974, https://doi.org/10.1016/j.jaerosci.2022.105974, 2022.

Harold, S. E., Bready, C. J., Juechter, L. A., Kurfman, L. A., Vanovac, S., Fowler, V. R., Mazaleski, G. E., Odbadrakh, T. T., and Shields,

385

G. C.: Hydrogen-Bond Topology Is More Important Than Acid/Base Strength in Atmospheric Prenucleation Clusters, J. Phys. Chem. A, 126, 1718–1728, https://doi.org/10.1021/acs.jpca.1c10754, 2022.

Hasan, G., Wu, H., Knattrup, Y., and Elm, J.: Base Synergy in Freshly Nucleated Particles, Aerosol Research Discussions, pp. 1–19, https://doi.org/10.5194/ar-2024-28, 2024.

Hunter, E. P. L. and Lias, S. G.: Evaluated Gas Phase Basicities and Proton Affinities of Molecules: An Update, J. Phys. Chem. Ref. Data,

390

27, 413–656, https://doi.org/10.1063/1.556018, 1998.

Jen, C. N., McMurry, P. H., and Hanson, D. R.: Stabilization of Sulfuric Acid Dimers by Ammonia, Methylamine, Dimethylamine, and Trimethylamine, J. Geophys. Res. Atmos., 119, 7502–7514, https://doi.org/10.1002/2014JD021592, 2014.

Jokinen, T., Sipilä, M., Junninen, H., Ehn, M., Lönn, G., Hakala, J., Petäjä, T., Mauldin, R. L. I., Kulmala, M., and Worsnop, D. R.: Atmospheric Sulphuric Acid and Neutral Cluster Measurements using CI-APi-TOF, Atmos. Chem. Phys., 12, 4117–4125,

395

https://doi.org/10.5194/acp-12-4117-2012, 2012.

Kirkby, J., Curtius, J., Almeida, J., Dunne, E., Duplissy, J., Ehrhart, S., Franchin, A., Gagné, S., Ickes, L., Kürten, A., and et al.: Role of Sulphuric Acid, Ammonia and Galactic Cosmic Rays in Atmospheric Aerosol Nucleation, Nature, 476, 429–433, https://doi.org/10.1038/nature10343, 2011.

Knattrup, Y. and Elm, J.: Clusteromics IV: The Role of Nitric Acid in Atmospheric Cluster Formation, ACS Omega, 7, 31 551–31 560,

400

https://doi.org/10.1021/acsomega.2c04278, 2022.

Knattrup, Y., Kubečka, J., and Elm, J.: Nitric Acid and Organic Acids Suppress the Role of Methanesulfonic Acid in Atmospheric New Particle Formation, J. Phys. Chem. A, 127, 7568–7578, https://doi.org/10.1021/acs.jpca.3c04393, 2023.

Knattrup, Y., Kubečka, J., Wu, H., Jensen, F., and Elm, J.: Reparameterization of GFN1-xTB for Atmospheric Molecular Clusters: Applications to Multi-Acid–Multi-Base Systems, RSC Adv., 14, 20 048–20 055, https://doi.org/10.1039/D4RA03021D, 2024.

405 Kristensen, K., Enggrob, K. L., King, S. M., Worton, D. R., Platt, S. M., Mortensen, R., Rosenoern, T., Surratt, J. D., Bilde, M., Goldstein, A. H., and Glasius, M.: Formation and Occurrence of Dimer Esters of Pinene Oxidation Products in Atmospheric Aerosols, Atmos. Chem. Phys., 13, 3763–3776, https://doi.org/10.5194/acp-13-3763-2013, 2013.

Kristensen, K., Watne, Å. K., Hammes, J., Lutz, A., Petäjä, T., Hallquist, M., Bilde, M., and Glasius, M.: High-Molecular Weight Dimer Esters Are Major Products in Aerosols from $\alpha$-Pinene Ozonolysis and the Boreal Forest, Environ. Sci. Technol. Lett., 3, 280–285,
410 https://doi.org/10.1021/acs.estlett.6b00152, 2016.

Kubečka, J., Besel, V., Neefjes, I., Knattrup, Y., Kurtén, T., Vehkamäki, H., and Elm, J.: Computational Tools for Handling Molecular Clusters: Configurational Sampling, Storage, Analysis, and Machine Learning, ACS Omega, 8, 45 115–45 128, https://doi.org/10.1021/acsomega.3c07412, 2023a.

Kubečka, J., Neefjes, I., Besel, V., Qiao, F., Xie, H.-B., and Elm, J.: Atmospheric Sulfuric Acid–Multi-Base New Particle Formation Revealed
415 through Quantum Chemistry Enhanced by Machine Learning, J. Phys. Chem. A, 27, 2091–2103, https://doi.org/10.1021/acs.jpca.3c00068, 2023b.

Kulmala, M., Kontkanen, J., Junninen, H., Lehtipalo, K., Manninen, H. E., Nieminen, T., Petäjä, T., Sipilä, M., Schobesberger, S., Rantala, P., and et al.: Direct Observations of Atmospheric Aerosol Nucleation, Science, 339, 943–946, https://doi.org/10.1126/science.1227385, 2013.

420 Kumar, M., Li, H., Zhang, X., Zeng, X. C., and Francisco, J. S.: Nitric Acid–Amine Chemistry in the Gas Phase and at the Air–Water Interface, J. Am. Chem. Soc., 140, 6456–6466, https://doi.org/10.1021/jacs.8b03300, 2018.

Kurtén, T., Loukonen, V., Vehkamäki, H., and Kulmala, M.: Amines are Likely to Enhance Neutral and Ion-Induced Sulfuric Acid-Water Nucleation in the Atmosphere more Effectively than Ammonia, Atmos. Chem. Phys., 8, 4095–4103, https://doi.org/10.5194/acp-8-4095-2008, 2008.

425 Kurtén, T., Tiusanen, K., Roldin, P., Rissanen, M., Luy, J.-N., Boy, M., Ehn, M., and Donahue, N.: $\alpha$-Pinene Autoxidation Products May Not Have Extremely Low Saturation Vapor Pressures Despite High O:C Ratios, J. Phys. Chem. A, 120, 2569–2582, https://doi.org/10.1021/acs.jpca.6b02196, 2016.

Ling, J., Ding, X., Li, Z., and Yang, J.: First-Principles Study of Molecular Clusters Formed by Nitric Acid and Ammonia, J. Phys. Chem. A, 121, 661–668, https://doi.org/10.1021/acs.jpca.6b09185, 2017.

430 Liu, L., Li, H., Zhang, H., Zhong, J., Bai, Y., Ge, M., Li, Z., Chen, Y., and Zhang, X.: The role of Nitric Acid in Atmospheric New Particle Formation, Phys. Chem. Chem. Phys., 20, 17 406–17 414, https://doi.org/10.1039/C8CP02719F, 2018.

Liu, L., Yu, F., Du, L., Yang, Z., Francisco, J. S., and Zhang, X.: Rapid Sulfuric Acid–Dimethylamine Nucleation Enhanced by Nitric Acid in Polluted Regions, Proc. Natl. Acad. Sci. U.S.A., 118, e2108384 118, https://doi.org/10.1073/pnas.2108384118, 2021.

Longsworth, O. M., Bready, C. J., Joines, M. S., and Shields, G. C.: The Driving Effects of Common Atmospheric Molecules for Formation
435 of Clusters: The Case of Sulfuric Acid, Nitric Acid, Hydrochloric Acid, Ammonia, and Dimethylamine, Environ. Sci.: Atmos., 3, 1585–1600, https://doi.org/10.1039/D3EA00118K, 2023.

Loukonen, V., Kurtén, T., Ortega, I. K., Vehkamäki, H., Pádua, A. A. H., Sellegri, K., and Kulmala, M.: Enhancing Effect of Dimethylamine in Sulfuric Acid Nucleation in the Presence of Water – a Computational Study, Atmos. Chem. Phys., 10, 4961–4974, https://doi.org/10.5194/acp-10-4961-2010, 2010.

440 Merikanto, J., Spracklen, D. V., Mann, G. W., Pickering, S. J., and Carslaw, K. S.: Impact of Nucleation on Global CCN, Atmos. Chem. Phys., 9, 8601–8616, https://doi.org/10.5194/acp-9-8601-2009, 2009.

Nadykto, A. B. and Yu, F.: Strong Hydrogen Bonding between Atmospheric Nucleation Precursors and common Organics, Chem. Phys. Lett., 435, 14–18, https://doi.org/10.1016/j.cplett.2006.12.050, 2007.

Nadykto, A. B., Yu, F., Jakovleva, M. V., Herb, J., and Xu, Y.: Amines in the Earth's Atmosphere: A Density Functional Theory Study of the
445 Thermochemistry of Pre-Nucleation Clusters, Entropy, 13, 554–569, https://doi.org/10.3390/e13020554, 2011.

Nadykto, A. B., Herb, J., Yu, F., and Xu, Y.: Enhancement in the Production of Nucleating Clusters due to Dimethylamine and Large Uncertainties in the Thermochemistry of Amine-Enhanced Nucleation, Chem. Phys. Lett., 609, 42–49, https://doi.org/10.1016/j.cplett.2014.03.036, 2014.

Nadykto, A. B., Herb, J., Yu, F., Xu, Y., and Nazarenko, E. S.: Estimating the Lower Limit of the Impact of Amines on Nucleation in the
450 Earth's Atmosphere, Entropy, 17, 2764–2780, https://doi.org/10.3390/e17052764, 2015.

Najibi, A. and Goerigk, L.: The Nonlocal Kernel in van der Waals Density Functionals as an Additive Correction: An Extensive Analysis with Special Emphasis on the B97M-V and $\omega$B97M-V Approaches, J. Chem. Theory Comput., 14, 5725–5738, https://doi.org/10.1021/acs.jctc.8b00842, 2018.

Neese, F.: The ORCA Program System, WIREs Comput. Mol. Sci., 2, 73–78, https://doi.org/10.1002/wcms.81, 2012.

455 Neese, F.: Software Update: The ORCA Program System—Version 5.0, WIREs Comput. Mol. Sci., 12, e1606, https://doi.org/10.1002/wcms.1606, 2022.

Neese, F., Wennmohs, F., Becker, U., and Riplinger, C.: The ORCA Quantum Chemistry Program Package, J. Chem. Phys., 152, https://doi.org/10.1063/5.0004608, 2020.

Nguyen, M.-T., Jamka, A. J., Cazar, R. A., and Tao, F.-M.: Structure and Stability of the Nitric Acid–Ammonia Complex in the Gas Phase
460 and in Water, J. Chem. Phys., 106, 8710–8717, https://doi.org/10.1063/1.473925, 1997.

Nozière, B., Kalberer, M., Claeys, M., Allan, J., D'Anna, B., Decesari, S., Finessi, E., Glasius, M., Grgić, I., Hamilton, J. F., and et al.: The Molecular Identification of Organic Compounds in the Atmosphere: State of the Art and Challenges, Chem. Rev., 115, 3919–3983, https://doi.org/10.1021/cr5003485, 2015.

Passananti, M., Zapadinsky, E., Zanca, T., Kangasluoma, J., Myllys, N., Rissanen, M. P., Kurtén, T., Ehn, M., Attoui, M., and
465 Vehkamäki, H.: How Well can we Predict Cluster Fragmentation inside a Mass Spectrometer?, Chem. Commun., 55, 5946–5949, https://doi.org/10.1039/C9CC02896J, 2019.

Pedersen, A. N., Knattrup, Y., and Elm, J.: A cluster-of-functional-groups approach for studying organic enhanced atmospheric cluster formation, Aerosol Research, 2, 123–134, https://doi.org/10.5194/ar-2-123-2024, 2024.

Pracht, P., Bohle, F., and Grimme, S.: Automated Exploration of the Low-Energy Chemical Space with Fast Quantum Chemical Methods,
470 Phys. Chem. Chem. Phys., 22, 7169–7192, https://doi.org/10.1039/C9CP06869D, 2020.

Qiao, F., Zhang, R., Zhao, Q., Ma, F., Chen, J., and Xie, H.-B.: A Surprisingly High Enhancing Potential of Nitric Acid in Sulfuric Acid–Methylamine Nucleation, Atmosphere, 15, 467, https://doi.org/10.3390/atmos15040467, 2024.

Schobesberger, S., Junninen, H., Bianchi, F., Lönn, G., Ehn, M., Lehtipalo, K., Dommen, J., Ehrhart, S., Ortega, I. K., Franchin, A., and et al.: Molecular Understanding of Atmospheric Particle Formation from Sulfuric Acid and Large Oxidized Organic Molecules, Proc. Natl. Acad. Sci. U.S.A., 110, 17 223–17 228, https://doi.org/10.1073/pnas.1306973110, 2013.

Stolzenburg, D., Fischer, L., Vogel, A. L., Heinritzi, M., Schervish, M., Simon, M., Wagner, A. C., Dada, L., Ahonen, L. R., Amorim, A., and et al.: Rapid Growth of Organic Aerosol Nanoparticles over a Wide Tropospheric Temperature Range, Proc. Natl. Acad. Sci. U.S.A., 115, 9122–9127, https://doi.org/10.1073/pnas.1807604115, 2018.

Tröstl, J., Chuang, W. K., Gordon, H., Heinritzi, M., Yan, C., Molteni, U., Ahlm, L., Frege, C., Bianchi, F., Wagner, R., and et al.: The Role of Low-Volatility Organic Compounds in Initial Particle Growth in the Atmosphere, Nature, 533, 527–531, https://doi.org/10.1038/nature18271, 2016.

Wang, M., Kong, W., Marten, R., He, X.-C., Chen, D., Pfeifer, J., Heitto, A., Kontkanen, J., Dada, L., Kürten, A., and et al.: Rapid Growth of New Atmospheric Particles by Nitric Acid and Ammonia Condensation, Nature, 581, 184–189, https://doi.org/10.1038/s41586-020-2270-4, 2020.

Wang, M., Xiao, M., Bertozzi, B., Marie, G., Rörup, B., Schulze, B., Bardakov, R., He, X.-C., Shen, J., Scholz, W., and et al.: Synergistic HNO3–H2SO4–NH3 Upper Tropospheric Particle Formation, Nature, 605, 483–489, https://doi.org/10.1038/s41586-022-04605-4, 2022.

Weber, R. J., Marti, J. J., Mcmurry, P. H., Eisele, F. L., Tanner, D. J., and Jefferson, A.: Measured Atmospheric New Particle Formation Rates: Implications for Nucleation Mechanisms, Chem. Eng. Commun., pp. 53–64, https://www.tandfonline.com/doi/abs/10.1080/00986449608936541, 1996.

Wu, H., Engsvang, M., Knattrup, Y., Kubečka, J., and Elm, J.: Improved Configurational Sampling Protocol for Large Atmospheric Molecular Clusters, ACS Omega, 8, 45 065–45 077, https://doi.org/10.1021/acsomega.3c06794, 2023.

Wu, H., Knattrup, Y., Jensen, A. B., and Elm, J.: Cluster-to-Particle Transition in Atmospheric Nanoclusters, Aerosol Research Discussions, pp. 1–20, https://doi.org/10.5194/ar-2024-16, 2024.

Zapadinsky, E., Passananti, M., Myllys, N., Kurtén, T., and Vehkamäki, H.: Modeling on Fragmentation of Clusters inside a Mass Spectrometer, J. Phys. Chem. A, 123, 611–624, https://doi.org/10.1021/acs.jpca.8b10744, 2019.

Zhang, J.: Atom Typing using Graph Representation Learning: How do Models Learn Chemistry?, J. Chem. Phys., 156, 204 108, https://doi.org/10.1063/5.0095008, 2022.

Zhang, J. and Dolg, M.: ABCluster: The Artificial Bee Colony Algorithm for Cluster Global Optimization, Phys. Chem. Chem. Phys., 17, 24 173–24 181, https://doi.org/10.1039/C5CP04060D, 2015.

Zhang, J. and Dolg, M.: Global Optimization of Clusters of Rigid Molecules using the Artificial Bee Colony Algorithm, Phys. Chem. Chem. Phys., 18, 3003–3010, https://doi.org/10.1039/C5CP06313B, 2016.

Zhang, R., Jiang, S., Liu, Y.-R., Wen, H., Feng, Y.-J., Huang, T., and Huang, W.: An Investigation about the Structures, Thermodynamics and Kinetics of the Formic Acid involved Molecular Clusters, Chem. Phys., 507, 44–50, https://doi.org/10.1016/j.chemphys.2018.03.029, 2018.

Zhang, R., Shen, J., Xie, H.-B., Chen, J., and Elm, J.: The Role of Organic Acids in New Particle Formation from Methanesulfonic Acid and Methylamine, Atmos. Chem. Phys., 22, 2639–2650, https://doi.org/10.5194/acp-22-2639-2022, 2022.

Zhao, B., Donahue, N. M., Zhang, K., Mao, L., Shrivastava, M., Ma, P.-L., Shen, J., Wang, S., Sun, J., Gordon, H., and et al.: Global Variability in Atmospheric New Particle Formation mechanisms, Nature, 631, 98–105, https://doi.org/10.1038/s41586-024-07547-1, 2024.